Development 135, 1427-1437 (2008) doi:10.1242/dev.012922

A core cochlear phenotype in USH1 mouse mutants implicates fibrous links of the hair bundle in its cohesion, orientation and differential growth

Gaelle Lefèvre[1], Vincent Michel[1], Dominique Weil[1], Léa Lepelletier[1], Emilie Bizard[1], Uwe Wolfrum[2], Jean-Pierre Hardelin[1] and Christine Petit[1,3,*]

The planar polarity and staircase-like pattern of the hair bundle are essential to the mechanoelectrical transduction function of inner ear sensory cells. Mutations in genes encoding myosin VIIa, harmonin, cadherin 23, protocadherin 15 or sans cause Usher syndrome type I (USH1, characterized by congenital deafness, vestibular dysfunction and retinitis pigmentosa leading to blindness) in humans and hair bundle disorganization in mice. Whether the USH1 proteins are involved in common hair bundle morphogenetic processes is unknown. Here, we show that mouse models for the five USH1 genetic forms share hair bundle morphological defects. Hair bundle fragmentation and misorientation (25-52° mean kinociliary deviation, depending on the mutant) were detected as early as embryonic day 17. Abnormal differential elongation of stereocilia rows occurred in the first postnatal days. In the emerging hair bundles, myosin VIIa, the actin-binding submembrane protein harmonin-b, and the interstereocilia-kinocilium lateral link components cadherin 23 and protocadherin 15, all concentrated at stereocilia tips, in accordance with their known in vitro interactions. Soon after birth, harmonin-b switched from the tip of the stereocilia to the upper end of the tip link, which also comprises cadherin 23 and protocadherin 15. This positional change did not occur in mice deficient for cadherin 23 or protocadherin 15. We suggest that tension forces applied to the early lateral links and to the tip link, both of which can be anchored to actin filaments via harmonin-b, play a key role in hair bundle cohesion and proper orientation for the former, and in stereociliary elongation for the latter.

KEY WORDS: Usher syndrome, Hair bundle links, Planar polarity, Stereocilia growth, Harmonin (USH1C), Cadherin 23 (USH1D), Protocadherin 15 (USH1F), Sans (USH1G), Myosin VII (USH1B)

INTRODUCTION

Usher syndrome (USH) is the most frequent cause of hereditary deaf-blindness in humans. Of the three clinical forms (USH1-3), USH1 is the most severe. It is characterized by severe to profound congenital hearing impairment, constant vestibular dysfunction and pre-pubertal onset retinitis pigmentosa. Five *USH1* genes have been identified. They encode the unconventional myosin VIIa (*USH1B*), the PDZ-domain-containing scaffold protein harmonin (*USH1C*), cadherin 23 (*USH1D*) and protocadherin 15 (*USH1F*), which are two cadherins with long extracellular regions, and the protein sans (*USH1G*), which contains ankyrin repeats and a sterile alpha motif (Fig. 1A) (Ahmed et al., 2001; Alagramam et al., 2001b; Bitner-Glindzicz et al., 2000; Bolz et al., 2001; Bork et al., 2001; Verpy et al., 2000; Weil et al., 1995; Weil et al., 2003).

The cochlear and vestibular sensory cells (hair cells) respond to sound and head movements, respectively. The hair bundle located at their apex is the mechanosensitive organelle. The cochlear hair bundle consists of three to four graded rows of F-actin-filled, large and stiff microvilli, known as stereocilia, which are interconnected by fibrous links and together form a 'V'-shaped staircase (Fig. 1B). During its development, the cochlear hair bundle also includes a single transient genuine cilium, the kinocilium, which is located at the vertex of the 'V' and is also connected to the tallest stereocilia row by fibrous links (Fig. 1B). All vertices of cochlear hair bundles point to the lateral wall of the cochlear duct, thereby defining the planar cell polarity (PCP) axis of the sensory epithelium (organ of Corti) (Fig. 1B). Such an organization allows the uniform deflection of hair bundles along the PCP axis in response to a sound stimulus. Indeed, deflection along this axis, which is also the hair bundle symmetry axis, is the only effective direction to gate the mechanoelectrical transducer ion channels. According to the 'gating spring' model, hair bundle deflection towards the tallest row of stereocilia stretches the tip link (a single apical link that connects the tip of each stereocilium to the side of its adjacent taller neighbor). This in turn opens the transduction channel that is tethered to this link and causes hair cell depolarization (Hudspeth, 1985). Increasing evidence indicates that cadherin 23 and protocadherin 15 make up the upper and lower parts of the tip link, respectively (Ahmed et al., 2006; Kazmierczak et al., 2007; Siemens et al., 2004).

Disorganization of the inner ear hair bundles has been observed in spontaneous mouse mutants carrying allelic variants of each *USH1* gene ortholog, namely shaker 1 (*Myo7a*^{sh1}), deaf circler (*Ush1c*^{dfcr}), waltzer (*Cdh23*^{v}), Ames waltzer (*Pcdh15*^{av}) and Jackson shaker (*Ush1g*^{js}) (Alagramam et al., 2001a; Di Palma et al., 2001; Gibson et al., 1995; Johnson et al., 2003; Kikkawa et al., 2003; Kitamura et al., 1992; Pawlowski et al., 2006; Wilson et al., 2001). The abnormal hair bundle architecture of these mutants accounts for their hearing and balance impairments. In addition, it has led to discovery of the existence of transient lateral links that connect the stereocilia together and with the kinocilium during early hair bundle development (Goodyear et al., 2005). Some of these links are indeed composed of cadherin 23 (Michel et al., 2005) and protocadherin 15 (Ahmed et al., 2006). The role played by these early connectors in

[1]Unité de Génétique des Déficits Sensoriels, UMRS587 INSERM-Université Paris VI, Institut Pasteur, 25 rue du Dr Roux, 75724 Paris cedex 15, France. [2]Johannes Gutenberg University of Mainz, Institute of Zoology, Cell and Matrix Biology, Muellerweg 6, D-55099 Mainz, Germany. [3]Collège de France, 11 place Marcellin Berthelot, 75231 Paris cedex 05, France.

*Author for correspondence (email: cpetit@pasteur.fr)

Accepted 7 February 2008

the differentiation of the hair bundle is, however, poorly understood. A scaffolding role has been ascribed to harmonin, as its PDZ domains are expected to allow the formation of large molecular complexes. Myosin VIIa is an actin filament plus-end-directed myosin, which is therefore expected to move from the base to the apex of stereocilia. Moreover, genetic evidence supports its involvement in the targeting of various hair bundle proteins, including harmonin, during postnatal stages (Boeda et al., 2002; Michalski et al., 2007; Senften et al., 2006).

Several in vitro interactions between USH1 proteins have been reported (Fig. 1C). Harmonin can bind to the four other USH1 proteins (Adato et al., 2005; Boeda et al., 2002; Reiners et al., 2005; Siemens et al., 2002; Weil et al., 2003), and myosin VIIa can interact with sans and protocadherin 15 (Adato et al., 2005; Senften et al., 2006). By contrast, only sparse evidence has been collected to support direct interactions between these proteins within the hair bundle. In addition, the precise developmental processes in which these proteins are involved are still unknown. We addressed these issues by searching for common hair bundle anomalies in mouse models for each of the five USH1 genetic forms, and by investigating the possible co-distributions and interdependent localizations of the Ush1 proteins.

MATERIALS AND METHODS

Animals and antibodies

Cdh23$^{v2J/v2J}$, *Pcdh15*$^{av3J/av3J}$ and *Ush1g*$^{js/js}$ mice were obtained from Jackson Laboratories (Bar Arbor, ME). *Myo7a*$^{4626SB/4626SB}$ mice were kindly provided by Dr K. P. Steel (Sanger Institute, Cambridge, UK), and we produced *Ush1c* knockout mice (referred to as *Ush1c*$^{-/-}$) (see Fig. S1 in the supplementary material). Embryonic day 0 (E0) was determined by vaginal plug detection, and the day of birth was considered P0. In all procedures, mice were treated in accordance with both INSERM and Pasteur Institute welfare guidelines.

Rabbit polyclonal antibodies used to detect myosin VIIa (here named Myo7a-F1; 1:1000), harmonin-b (harmonin-H1b; 1:100), cadherin 23a (Cdh23-N1; 1:100) and protocadherin 15a/b (here named Pcdh15-cter; 1:500) have been described (Boeda et al., 2002; el-Amraoui et al., 1996; Reiners et al., 2005). The rabbit anti-Vangl2 antibody (1:200) was kindly provided by Drs Yao and Noda (JFCR Cancer Institute, Tokyo, Japan). Additional antibodies are commercially available: goat anti-Scrib1 (1:100; Santa Cruz Biotechnology, Santa Cruz, CA), rabbit anti-frizzled 3 (1:200; Sigma, Evry, France), mouse anti-β-catenin (1:200; Transduction Laboratories, BD Biosciences, Le Pont de Claix, France), mouse anti-acetylated-tubulin (1:200; Sigma), Alexa Fluor 488 or 546 F(ab′)$_2$ fragment of goat anti-rabbit IgG, Alexa Fluor 488 F(ab′)$_2$ fragment of goat anti-mouse IgG, Alexa Fluor 488 donkey anti-goat IgG (1:500; Molecular Probes-Invitrogen, Cergy Pontoise, France) and TRITC-conjugated phalloidin (1:1000; Sigma).

Whole-mount immunofluorescence

Mouse inner ears were dissected from temporal bones at different developmental stages. The cochlear shell was pierced at its apex, and the round and oval windows opened. Generally, inner ears were then immersed for fixation in 4% paraformaldehyde in PBS for 1 hour. After several washes in PBS, the cochlear shell was finely dissected and the organ of Corti processed as described (Michel et al., 2005). For Vangl2, the cochlear shell was dissected prior to fixation and the organ of Corti was only quickly fixed for 5 minutes in cold (–20°C) methanol. In this staining procedure, an anti-β-catenin antibody was used to label the apical region of hair cells because methanol has deleterious effects on the actin cytoskeleton. Fluorescence images were obtained with a confocal microscope (Zeiss LSM 510 META) equipped with a Plan Apochromat 63×/1.4 oil immersion objective. *z*-stack images were deconvoluted and reconstructed with Huygens (Scientific Volume Imaging, Hilversum, The Netherlands) and Image J (Rasband WS, US NIH, Bethesda, MD; http://rsb.info.nih.gov/ij/) software, respectively.

Scanning electron microscopy

Inner ears of *Ush1* mutant mice were processed as for immunofluorescence, except that they were fixed by immersion in 2.5% glutaraldehyde in 0.1 M phosphate buffer (pH 7.3) at room temperature for 2 hours. After several washes with buffer alone, they were finely dissected to provide direct access to the cochlear and vestibular sensory areas. The samples were then dehydrated by successive washes in ethanol (50, 70, 80, 90 and 100%), critical-point dried, mounted on a stub, sputter-coated with gold-palladium and examined under a Jeol JSM6700F scanning electron microscope.

Angular deviations were measured between the expected and effective positions of the kinocilia at the apical surfaces of hair cells from the cochlear apical turn, using the graphic tools of the Jeol JSM6700F software. Briefly, for each hair cell, the kinociliary deviation was determined by the angle formed by two crossing lines. The first line was drawn mediolaterally along the symmetry/PCP axis of the cell, thereby running through the expected position of the kinocilium. The second line was traced between the center of the hair cell surface and the effective position of the kinocilium. Data were analyzed using Excel (Microsoft).

RESULTS

Among the various mouse mutants identified for each *Ush1* gene, at least one carries a mutation with a predicted effect similar to that expected in the corresponding human USH1 form, except for USH1C. Indeed, the two *Ush1c* mouse mutants, *Ush1c*$^{dfcr/dfcr}$ and *Ush1c*$^{dfcr-2J/dfcr-2J}$, carry mutations that affect only some harmonin isoforms (Johnson et al., 2003), whereas virtually all *USH1C* mutations reported so far in patients are expected to be ‘functional null alleles’ (Bitner-Glindzicz et al., 2000; Verpy et al., 2000; Zwaenepoel et al., 2001). Therefore, we engineered a harmonin-null (*Ush1c*$^{-/-}$) mouse lacking *Ush1c* exon 1, which contains the translation initiation site common to all reported harmonin isoforms (see Fig. S1 in the supplementary material).

Ush1 mutant mice exhibit fragmented and misoriented hair bundles from E17.5 onwards

In the mouse cochlea, postmitotic cells of the primordial sensory epithelium differentiate in concurrent medial-to-lateral (neural-to-abneural) and basal-to-apical gradients along the cochlear duct between E14.5 and 18.5. Sensory cells concomitantly become organized into one row of inner hair cells (IHCs, the genuine sensory cells) and three rows of outer hair cells (OHCs, the cochlear amplifiers) (Fig. 1B), by cell intercalations. This convergent extension process results in the shortening in width and extension in length of the sensory epithelium. Actin-rich protrusions, which will ultimately form the stereocilia, soon emerge at the hair cell apical surface (Chen and Segil, 1999; Lim and Anniko, 1985; Sher, 1971). In the mouse, temporal information regarding the differentiation of these protrusions into fully mature stereocilia is limited. In the rat and hamster, the protrusions rapidly assemble into a bundle and grow uniformly until late embryonic stages. Then, the growing stereocilia elongate differentially according to their location within the bundle, so that the staircase-like pattern of the stereocilia rows is settled a few days after birth. While supernumerary stereocilia are reabsorbed, the remaining stereocilia continue to grow simultaneously in length and width, until the hair bundle reaches its mature shape (Kaltenbach et al., 1994; Zine and Romand, 1996). Therefore, initial, intermediate and final periods of hair bundle development can be distinguished, in which the growth of the stereocilia row is uniform, differential and simultaneous, respectively. From our observations (see below), we established that the first two periods extend from E15.5 to P0, and from P1 to around P5, respectively, whereas the third lasts until P15, in the mouse. To determine and characterize hair bundle morphogenetic defects in

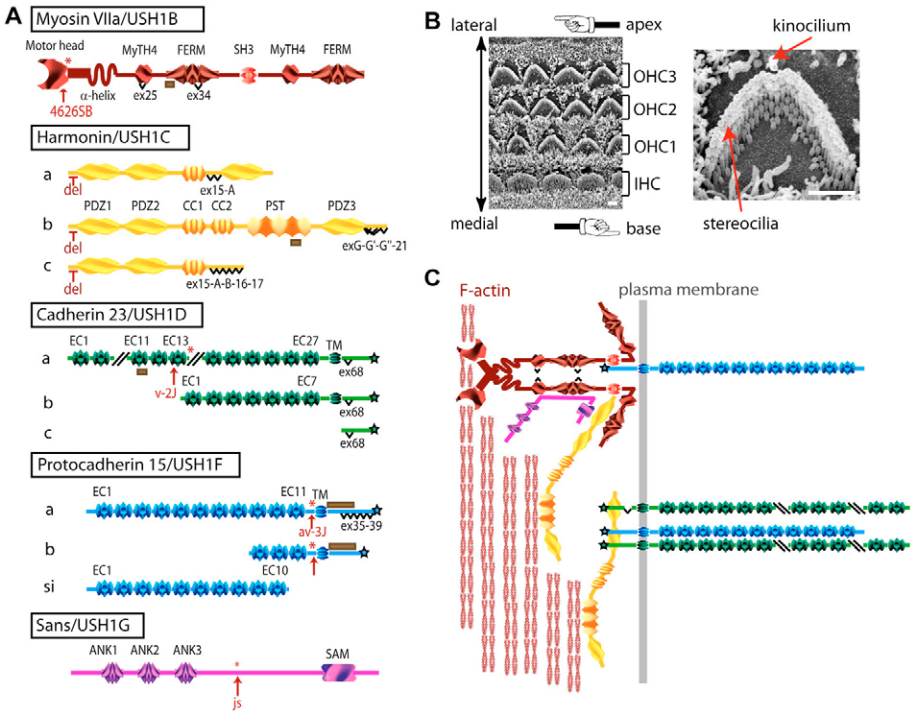

Fig. 1. The USH1 proteins and their interactions in vitro. (**A**) Predicted structures of the different USH1 protein isoforms. Myosin VIIa consists of a motor head, a neck region with five isoleucine-glutamine (IQ) motifs, and a large tail comprising an α-helix domain and two repeats, each composed of a myosin tail homology 4 (MyTH4) domain and a 4.1 ezrin radixin moesin (FERM) domain, separated by a Src homology 3 (SH3) domain (Chen et al., 1996; Weil et al., 1995). There are three classes of harmonin isoforms (a, b and c) (Verpy et al., 2000). Harmonin-a and harmonin-c have three and two PDZ domains, respectively, and harmonin-a also has a coiled-coil (CC) domain. Harmonin-b has the same domains as harmonin-a, plus a second CC domain and a proline, serine and threonine (PST)-rich sequence. Cadherin 23 and protocadherin 15 isoforms are also grouped into three classes (Ahmed et al., 2006; Lagziel et al., 2005). Cadherin 23a, cadherin 23b, protocadherin 15a and protocadherin 15b are transmembrane isoforms, with 27, 7, 11 and 1 extracellular cadherin (EC) repeat, respectively. Cadherin 23c isoforms are cytoplasmic, whereas protocadherin 15si isoforms are secreted. Multiple splice variants have been identified for myosin VIIa, protocadherin 15a, and each isoform class of harmonin and cadherin 23 (alternative exons are indicated) (Ahmed et al., 2006; Ahmed et al., 2003; Chen et al., 1996; Lagziel et al., 2005; Michel et al., 2005; Reiners et al., 2003; Verpy et al., 2000; Weil et al., 1995). Finally, sans has three ankyrin (ANK)-like repeats and a sterile alpha motif (SAM) domain (Kikkawa et al., 2003; Weil et al., 2003). Sans does not have any known splice variants. The respective locations of the mutations of the five USH1 mouse models used in this study are indicated by arrows for point mutations, and by inhibition signs for the deletion (del) of the transcription start site. The resulting stop codons are indicated by asterisks. The immunogenic regions for the antibodies used in this study are indicated by brown boxes. (**B**) Apical views of the auditory epithelium of a P5 wild-type mouse by scanning electron microscopy (SEM). Sensory inner hair cells (IHCs) and outer hair cells (OHCs) are organized into a single medial-side row and three lateral-side rows, respectively (left panel). A hair bundle that consists of stereocilia and a single transient kinocilium is present on top of every hair cell (right). Scale bar: 1 μm. (**C**) Schematic representation of known in vitro interactions between the USH1 proteins. The domains involved in each interaction are drawn in close apposition. Harmonin can bind to any of the other USH1 proteins. Cadherin 23a and protocadherin 15a/b cytoplasmic regions interact with harmonin PDZ1 and/or PDZ2 domains (Adato et al., 2005; Boeda et al., 2002; Reiners et al., 2005; Siemens et al., 2002). The presence of a consensus PDZ-binding motif at the C-terminus of cadherin 23a and protocadherin 15a/b isoforms is indicated by a star. Through its cytoplasmic region, protocadherin 15a/b can also bind to the myosin VIIa SH3 domain (Senften et al., 2006). The harmonin PDZ1 domain can interact with the second MyTH4-FERM repeat of the myosin VIIa tail and the SAM domain of sans (Boeda et al., 2002; Weil et al., 2003). Finally, the central region of sans can bind to the first MyTH4-FERM repeat of myosin VIIa (Adato et al., 2005). Harmonin and sans can also form homodimers (not shown) (Adato et al., 2005).

mice defective in myosin VIIa (*Myo7a*$^{4626SB/4626SB}$), harmonin (*Ush1c*$^{-/-}$), cadherin 23 (*Cdh23*$^{v2J/v2J}$), protocadherin 15 (*Pcdh15*$^{av3J/av3J}$) and sans (*Ush1g*$^{js/js}$), we undertook a systematic and comparative analysis of the different *Ush1* mutant hair bundles during these three developmental periods.

By confocal microscopy, we observed that every mutant displayed disorganized, fragmented IHC and OHC hair bundles as early as E17.5 and E18.5, respectively (Fig. 2A). Scanning electron microscopy (SEM) on P0 organs of Corti showed that in *Ush1* mutants, stereocilia generally assembled into two to three clumps at the cell apical surface, instead of forming an integral, single 'V'-shaped bundle as in wild-type hair cells (Fig. 2B). Remarkably, although lateral links that connect stereocilia to each other along their shaft were observed in stereociliary clumps of all *Ush1* mutant mice, they seemed sparse compared with those of wild-type hair bundles and were also more frequently disrupted (Fig. 2C).

Examination by confocal microscopy of E18.5 cochleas stained with actin and microtubule markers revealed that a large proportion of the hair cells displayed a mispositioned kinocilium in *Ush1* mouse mutants (Fig. 3A and data not shown). Moreover, observation of *Ush1* mutant hair bundles by SEM at P0 showed that the stereociliary clumps were also often misoriented (Figs 2, 3). According to the current view, the kinocilium leads the

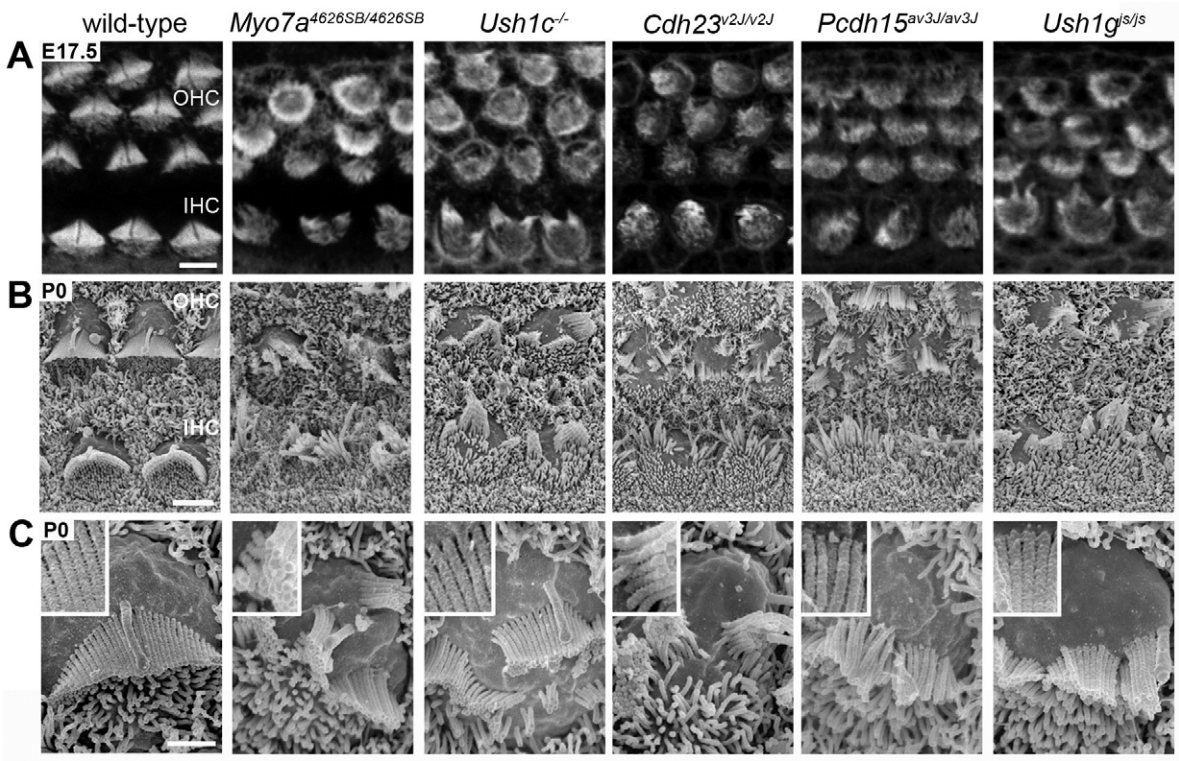

Fig. 2. Early fragmentation of *Ush1* mutant cochlear hair bundles during development. (**A**) Hair bundles of sensory cells from the cochlear basal turn of E17.5 wild-type and *Ush1* mutant mice. Whole-mounts of the organ of Corti were stained with phalloidin to reveal F-actin in stereocilia. (**B**) Analysis of P0 cochlear hair cells from wild-type and *Ush1* mutant mice by SEM. Note the fragmented aspect of the hair bundles, and sometimes also of the microvillar area, in the mutants. (**C**) OHC hair bundles in wild-type and *Ush1* mutant mice at P0. Lateral links are visible between stereocilia from both wild-type and mutant hair cells (see insets), although they appear sparser and frequently disrupted in the mutants, especially *Cdh23*$^{v2J/v2J}$ and *Pcdh15*$^{av3J/av3J}$. Scale bars: 2 μm in A,B; 1 μm in C.

establishment of the stereociliary bundle polarity (Jones and Chen, 2007). Therefore, we quantified the hair bundle polarity defect of the different *Ush1* mutants by measuring, on each hair cell surface, the kinocilium deviation (in degrees) from its expected position along the PCP axis (arbitrarily fixed as 0°) (Fig. 3B; see Materials and methods for details). Consistent with the previous study by Dabdoub et al. (Dabdoub et al., 2003), kinocilia had mean absolute deviations ranging from 6.5° in IHCs to 12.5° in OHCs of the third row in P0 wild-type mice. They were equally distributed on both sides of the PCP axis, and more than 80% of them were present within ±15° of the PCP axis (Fig. 3C and data not shown). By contrast, most hair cells of the *Ush1* mutants displayed mispositioned kinocilia. Both the IHCs and the three rows of OHCs showed larger mean kinociliary deviations than in wild-type mice (Fig. 3C). Only 37% of kinocilia at best (*Ush1g*$^{js/js}$), and 14% at worst (*Cdh23*$^{v2J/v2J}$), were present within ±15° of the PCP axis in the *Ush1* mutant hair cells (Fig. 3C). The mean absolute kinociliary deviations of IHCs and OHCs were 25° (*Ush1g*$^{js/js}$), 26° (*Myo7a*$^{4626SB/4626SB}$), 26° (*Ush1c*$^{-/-}$), 38° (*Pcdh15*$^{av3J/av3J}$) and 52° (*Cdh23*$^{v2J/v2J}$) (Fig. 3C). Nevertheless, virtually all kinocilia, apart from a small proportion in *Cdh23*$^{v2J/v2J}$ and *Pcdh15*$^{av3J/av3J}$ hair cells, were located within the lateral half and near the edge of the apical cell surface. Notably, in *Cdh23*$^{v2J/v2J}$ and *Pcdh15*$^{av3J/av3J}$ mice, the kinocilia were also often dissociated from the stereociliary clumps (Fig. 3C).

Recent studies have shown that the polarization of the kinocilium is secondary to the asymmetric distribution of core PCP proteins at cell-cell junctions of the hair cells (Deans et al., 2007). We therefore analyzed the distribution of two of these proteins, vang-like 2 (Vangl2) and frizzled 3, which are required for the establishment of inner ear PCP (Montcouquiol et al., 2003; Wang et al., 2006). In E18.5 *Ush1c*$^{-/-}$, *Cdh23*$^{v2J/v2J}$ and *Pcdh15*$^{av3J/av3J}$ mice, Vangl2 and frizzled 3 were asymmetrically distributed on the apical, medial side of hair cells, as in wild-type littermates (see Fig. S2 in the supplementary material). In addition, scribble 1 (Scrib1; scribbled), which has also been found to be involved in inner ear PCP (Montcouquiol et al., 2003), was normally distributed along the hair cell basolateral membrane in all *Ush1* mutant mice (see Fig. S2 in the supplementary material). Of note, PCP proteins are also required for cochlear convergent extension (Jones and Chen, 2007). In agreement with the normal distributions of Vangl2, frizzled 3 and Scrib1, organs of Corti in all *Ush1* mouse mutants had normal length and width at P0, and they did not show extra hair cell rows (data not shown).

Ush1 proteins localize at stereocilia tips during initial hair bundle development

The early core phenotype that we identified in *Ush1* mutant mice as early as E17.5 suggests that the Ush1 proteins cooperate during the initial period of hair bundle development. To determine whether Ush1 proteins colocalize during this period, we studied their distribution by immunofluorescence analysis of whole-mount cochleas. For each Ush1 protein, we focused on specific isoform classes that have been shown to be either prominent in, or largely restricted to, the inner ear and retina (Ahmed et al., 2006; Ahmed et al., 2003; Hasson et al., 1995; Lagziel et al., 2005; Michel et al.,

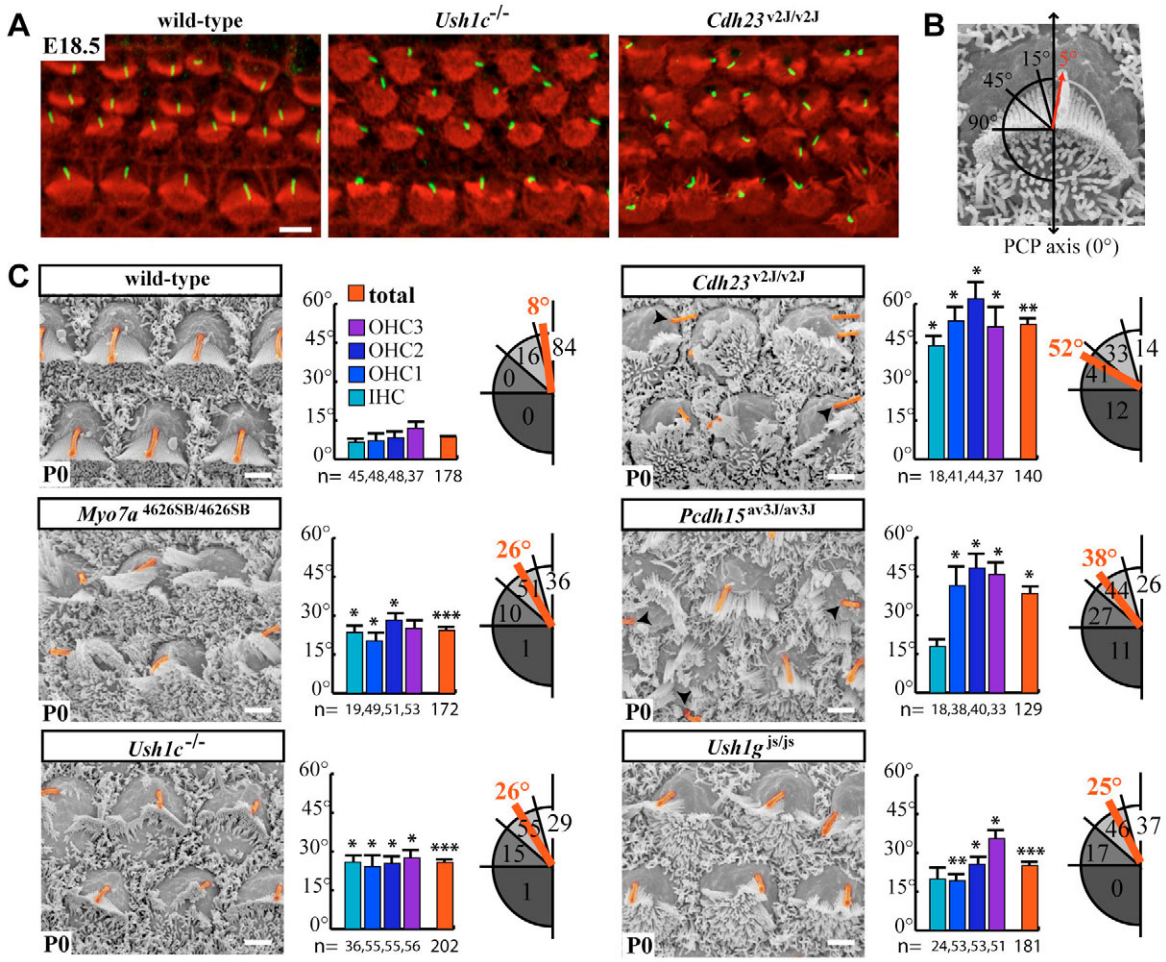

Fig. 3. Mispositioning of the kinocilium in *Ush1* mutant hair cells. (**A**) Basal view of E18.5 cochlear whole-mounts from wild-type, *Ush1c*$^{-/-}$ and *Cdh23*$^{v2J/v2J}$ mice were stained with an antibody that labels the kinocilia (green), and with phalloidin to reveal F-actin in stereocilia (red). (**B**) Schematic of the method used to measure the angular deviation of the kinocilium with respect to the PCP axis on SEM images. A P0 wild-type OHC is taken as an example. (**C**) Evaluation of the kinocilium position on P0 wild-type and *Ush1* mutant hair cells. For each mouse strain, kinocilia were falsely labeled orange (using Adobe Photoshop) to facilitate their visualization on SEM images of control and mutant OHCs. Mean absolute positions (±s.e.m.) of the kinocilia for the total population of hair cells (orange) and per hair cell row (blue to purple) are represented on the bar charts. *P*-values, which were determined with respect to the positions of kinocilia in wild-type mice using the Welch's *t*-test, are indicated by asterisks (*$P \leqslant 0.05$, **$P \leqslant 0.01$, ***$P \leqslant 0.001$). The pie charts present the percentage of hair cells in which the kinocilium is mispositioned by 0-14° (white), 15-44° (light-gray), 45-89° (medium-gray), or 90-180° (dark-gray) from its expected location at the lateral-most edge of the cell surface. Scale bars: 2 μm in A; 1 μm in C.

2005; Reiners et al., 2003; Rzadzinska et al., 2005; Verpy et al., 2000). Thus, submembrane actin-binding class b harmonin (harmonin-b), transmembrane class a cadherin 23 (cadherin 23a), transmembrane class a and class b protocadherin 15 (protocadherin 15a/b), and myosin VIIa isoforms were specifically stained by the harmonin-H1b, Cdh23-N1, Pcdh15-cter and Myo7a-F1 antibodies, respectively (Fig. 4). The specificity of these antibodies was established by the loss of hair bundle immunoreactivity in each mouse mutant deficient for the corresponding protein (see Fig. S3 in the supplementary material). In the absence of a similar specificity indication for our anti-sans antibody, we did not study the distribution of this protein.

Myosin VIIa, harmonin-b, cadherin 23a and protocadherin 15a/b were first detected in all the emerging protrusions of newly differentiated IHCs and OHCs from the cochlear basal turn at E15.5 and E16.5, respectively (Fig. 4 and data not shown). At these stages, the actin labeling did not enable discrimination of the future stereocilia from the surrounding microvilli. By E18.5, every hair cell along the cochlea stained positive for the four Ush1 proteins, which were all concentrated at the tips of both the differentiated stereocilia and surrounding microvilli (Fig. 4). Pcdh15-cter and Cdh23-N1 stainings also extended along the entire length of the stereocilia, and they were particularly intense in the region of the hair bundle where the stereocilia are connected to the kinocilium (Fig. 4).

Harmonin-b localization to the tips of emerging stereocilia is dependent on the presence of myosin VIIa and sans

The simultaneous presence of four Ush1 proteins at stereocilia tips during the initial phase of hair bundle morphogenesis, in conjunction with their well-documented in vitro interactions, suggested that they can interact during this period of development. Because of the central role played by harmonin in these in vitro interactions (Fig.

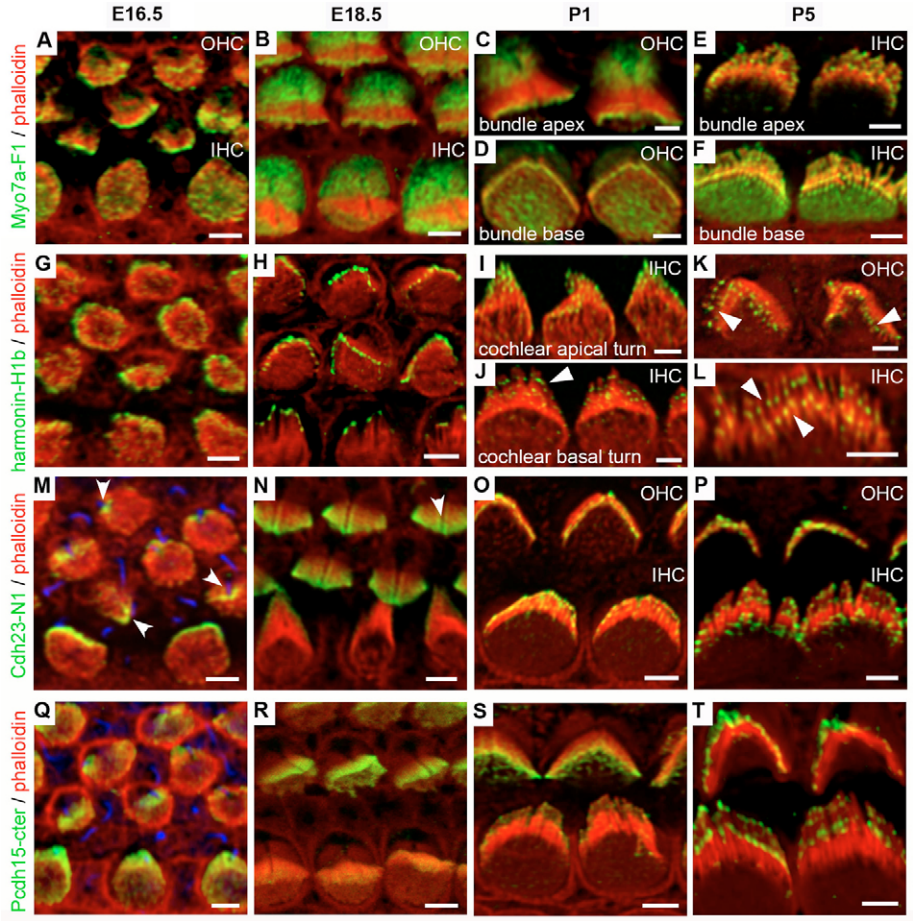

Fig. 4. Distribution of the mouse Ush1 proteins in wild-type hair bundles during development. Hair bundles from E16.5, E18.5, P1 and P5 wild-type mouse cochlear sensory cells stained with phalloidin (red) and antibodies to myosin VIIa (Myo7a-F1, **A-F**), harmonin-b (harmonin-H1b, **G-L**), cadherin 23a (Cdh23-N1, **M-P**), or protocadherin 15a/b (Pcdh15-cter, **Q-T**) (green). Unless otherwise stated, views are from the basal cochlear turn. At E16.5, the four Ush1 proteins are detected in the actin-rich protrusions that grow on top of the newly differentiated hair cells, with a particular concentration at their actin-free distal end (A,G,M,Q). Similar distribution patterns are also observed later, at E18.5, in the stereocilia and surrounding hair cell microvilli, which have become distinguishable by their different lengths (B,H,N,R). Note in M and N the strong Cdh23-N1 signals at the tip of the tallest protrusions adjacent to the kinocilia (arrowheads), which are stained for acetylated tubulin (blue) in M and Q. During postnatal stages, both Cdh23-N1 and Pcdh15-cter signals become restricted to stereocilia tips (O,P,S,T), whereas the harmonin-H1b signal is relocalized from the tip to the tip link upper insertion region in tall and medium stereocilia (arrowheads in J-L). A new Myo7a-F1 signal is detected near stereocilia bases during this period of hair bundle development (C-F), and the shafts of the growing stereocilia also stain positive for myosin VIIa (not shown). Scale bars: 2 μm.

1C) (Adato et al., 2005; Boeda et al., 2002; Reiners et al., 2005; Siemens et al., 2002; Weil et al., 2003), we further investigated the relationship between harmonin and the other Ush1 proteins. To this purpose, we analyzed the effect of the absence of harmonin on the distribution of myosin VIIa, cadherin 23a and protocadherin 15a/b, and analyzed the distribution of harmonin-b in the different *Ush1* mutants, during the initial period of hair bundle development, i.e. until P0.

The cadherin 23a and protocadherin 15a/b immunoreactivities were identical in wild-type and harmonin-null mice. Both Cdh23-N1 and Pcdh15-cter labelings became progressively restricted towards the distal ends of mutant and wild-type stereocilia (Fig. 5B). We did not detect any change in the distribution of harmonin-b at stereocilia tips in *Cdh23*$^{v2J/v2J}$ and *Pcdh15*$^{av3J/av3J}$ mice either (Fig. 5A). By contrast, hair bundles of the functionally null *Myo7a*$^{4626SB/4626SB}$ mutant failed to stain for harmonin-b as early as E17.5 (Fig. 5A). Instead, harmonin-b progressively accumulated below the hair bundles and formed immunoreactive bead-like foci from E18.5 onwards (Fig. 5A). Reciprocally, myosin VIIa was barely detectable at the stereocilia tips of E17.5 harmonin-null mice, although the weak staining observed along the stereocilia of wild-type mice persisted in the mutants (Fig. 5B). Finally, in sans-deficient *Ush1g*$^{js/js}$ mice, harmonin-b could not be detected within the hair bundles at any of the stages examined (from E17.5 to P0; Fig. 5A). Thus, from the earliest stages of cochlear hair bundle development, harmonin-b targeting to the stereocilia tips is dependent on both myosin VIIa and sans. In addition, myosin VIIa accumulation at the stereocilia tips is dependent on the presence of harmonin.

The intermediate phase of stereociliary growth is defective in *Ush1* mutant mice

Between P0 and P5, the three outward-most stereocilia rows of wild-type hair bundles showed differential row-specific elongation, ultimately leading to the characteristic staircase-like pattern of mature hair bundles (Fig. 6A). Strikingly, SEM analysis of *Ush1* mutant hair bundles during this period of development showed that many stereocilia were of abnormal length (Fig. 6A,B). Many stereocilia of *Myo7a*$^{4626SB/4626SB}$ mice were taller than those in wild-type mice (Fig. 6B). By contrast, in all the other *Ush1* mouse mutants, many stereocilia of the small and, to a lesser extent, medium rows were shorter than expected, whereas stereocilia of the tall row were of normal height (Fig. 6A,B). In particular, in OHCs defective in harmonin, the majority of stereocilia from the small and medium rows did not elongate further from P0. At P5 they were in the process of regressing, and at P15 they had disappeared (Fig. 6A).

As row-specific elongation proceeded, the tips of small and medium stereocilia evolved from a round, oblate shape into an asymmetric, prolate shape in wild-type hair bundles (Fig. 6C). Such a morphological change is thought to result from tension forces applied, via the tip link, to the apical membrane of these stereocilia (Rzadzinska et al., 2004). In *Ush1* mutant hair bundles, especially in IHCs, stereocilia of the small and medium rows virtually never had prolate tips, but rather had round, oblate tips (Fig. 6C), indicating that these putative tension forces might not develop properly in the absence of Ush1 proteins.

We therefore examined the distribution of interstereociliary links in the different *Ush1* mutant hair bundles. During late embryonic and early postnatal stages, the lateral fibrous links that are initially

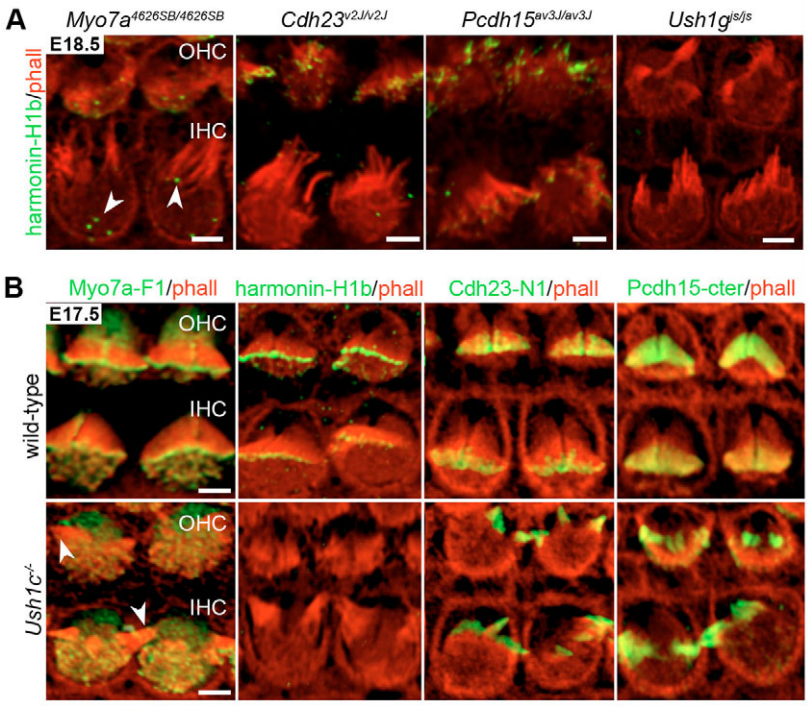

Fig. 5. Ush1 protein localization in early developing *Ush1* mutant hair bundles. (**A**) Hair bundles of sensory cells from the cochlear basal turn of E18.5 *Myo7a*$^{4626SB/4626SB}$, *Cdh23*$^{v2J/v2J}$, *Pcdh15*$^{av3J/av3J}$ and *Ush1g*$^{js/js}$ mice stained with the harmonin-H1b antibody (green) and phalloidin (red). Note the absence of signal in the hair bundles of *Ush1g*$^{js/js}$ and *Myo7a*$^{4626SB/4626SB}$ mice, and the presence of immunoreactive spots in the cuticular plate of the latter (arrowheads). (**B**) Hair bundles of sensory cells from the cochlear basal turn of E17.5 wild-type mice and *Ush1c*$^{-/-}$ mice that lack harmonin. Whole-mount cochleas were labeled with phalloidin (red) and antibodies to myosin VIIa (Myo7a-F1), harmonin-b (harmonin-H1b), cadherin 23a (Cdh23-N1) or protocadherin 15a/b (Pcdh15-cter) (green). Cdh23-a and Pcdh15-a/b are detected along the stereocilia shafts both in wild-type and *Ush1c*$^{-/-}$ hair bundles. Note the absence of a Myo7a-F1 signal at stereocilia tips in *Ush1c*$^{-/-}$ hair cells (arrowheads). Scale bars: 2 μm.

present all along the shafts of the growing stereocilia progressively become restricted towards the distal end of the stereocilia (forming apical lateral links), while two subsets of interstereociliary links can progressively be distinguished at their tips (tip links) and bases (ankle links) (Goodyear et al., 2005). Ankle links could be seen in most hair bundles of all *Ush1* mutants (data not shown), except *Myo7a*$^{4626SB/4626SB}$. This is consistent with the requirement of myosin VIIa for the stereociliary targeting of molecular components of the ankle links (Michalski et al., 2007). By contrast, in P5 *Cdh23*$^{v2J/v2J}$ and *Pcdh15*$^{av3J/av3J}$ mice, we failed to detect the presence of any apical (lateral or tip) links. In myosin VIIa-, harmonin- and sans-deficient mice, however, some of these links were still visible, but they appeared sparser than in wild-type mice (Fig. 6C).

Harmonin-b relocalization below stereocilia tips does not occur in cadherin 23- or protocadherin 15-defective mice

The additional phenotype that we identified in *Ush1* mutant mice during the period of differential stereociliary growth suggests that the Ush1 proteins also cooperate in this hair bundle morphogenetic step. Therefore, we examined whether myosin VIIa, harmonin-b, cadherin 23a and protocadherin 15a/b still colocalized in wild-type stereocilia during this period of hair bundle morphogenesis. From P0 onwards, both the Cdh23-N1 and Pcdh15-cter stainings became progressively restricted towards the distal part of the growing stereocilia, so that only stereocilia tips remained immunoreactive from P5 onwards (Fig. 4). The Cdh23-N1 labeling, however, was barely detectable after P13, indicating that our antibody fails to detect the tip link (data not shown). Meanwhile, the distribution profiles of myosin VIIa and harmonin-b underwent a dramatic change at P0 and P1, respectively. From P0 onwards, the myosin VIIa immunoreactivity of stereocilia tips progressively decreased and a new bright Myo7a-F1 staining was detected near the base of stereocilia (Fig. 4). Remarkably, from P1 and P4 onwards, harmonin-b was no longer detected at stereocilia tips of IHCs and OHCs, respectively. Instead, it was detected below the tip of tall and medium stereocilia, in single spots facing the tips of the adjacent shorter stereocilia, and not in the small stereocilia (Fig. 4). Notably, this region corresponds to the upper attachment point of the tip link. The distribution profile of harmonin-b then remained largely unchanged until hair bundles were fully mature (data not shown).

Remarkably, we observed that the harmonin-H1b immunoreactivity remained at stereocilia tips and was not detected in the region of the tip link upper end in P5 *Cdh23*$^{v2J/v2J}$ and *Pcdh15*$^{av3J/av3J}$ hair bundles (Fig. 7A), suggesting that the two cadherins directly or indirectly control the harmonin-b switch. By contrast, Cdh23-N1 and Pcdh15-cter labelings were detected at stereocilia tips in harmonin-null mice (Fig. 7B), as in wild-type mice. This suggests that cadherin 23a and protocadherin 15a/b do not rely on the presence of harmonin isoforms for their apical distribution. Whether they require harmonin to form functional apical links, however, remains to be examined. In *Myo7a*$^{4626SB/4626SB}$ and sans-deficient *Ush1g*$^{js/js}$ mice, harmonin-b was again not detected in the stereocilia (Fig. 7A).

DISCUSSION

In this study, we identified common morphological anomalies of developing hair bundles in mouse models for the five USH1 genetic forms. This core Ush1 phenotype includes the fragmentation and misorientation of hair bundles from the earliest stages of their development, as well as stereocilia elongation and apical tip defects at later stages.

Hair bundle polarization has been described as a two-step process. From E15.5 in the mouse, the kinocilium migrates towards a lateral position, from the center to the periphery of the cell apical surface. Then, once stereocilia have differentiated and assembled into a bundle, a reorientation step occurs in which the hair bundle progressively reaches its final location on the cell apical surface, pointing towards the distal pole (Cotanche and Corwin, 1991; Denman-Johnson and Forge, 1999; Dabdoub et al., 2003). The role of the kinocilium in the differentiation, growth and assembly of the

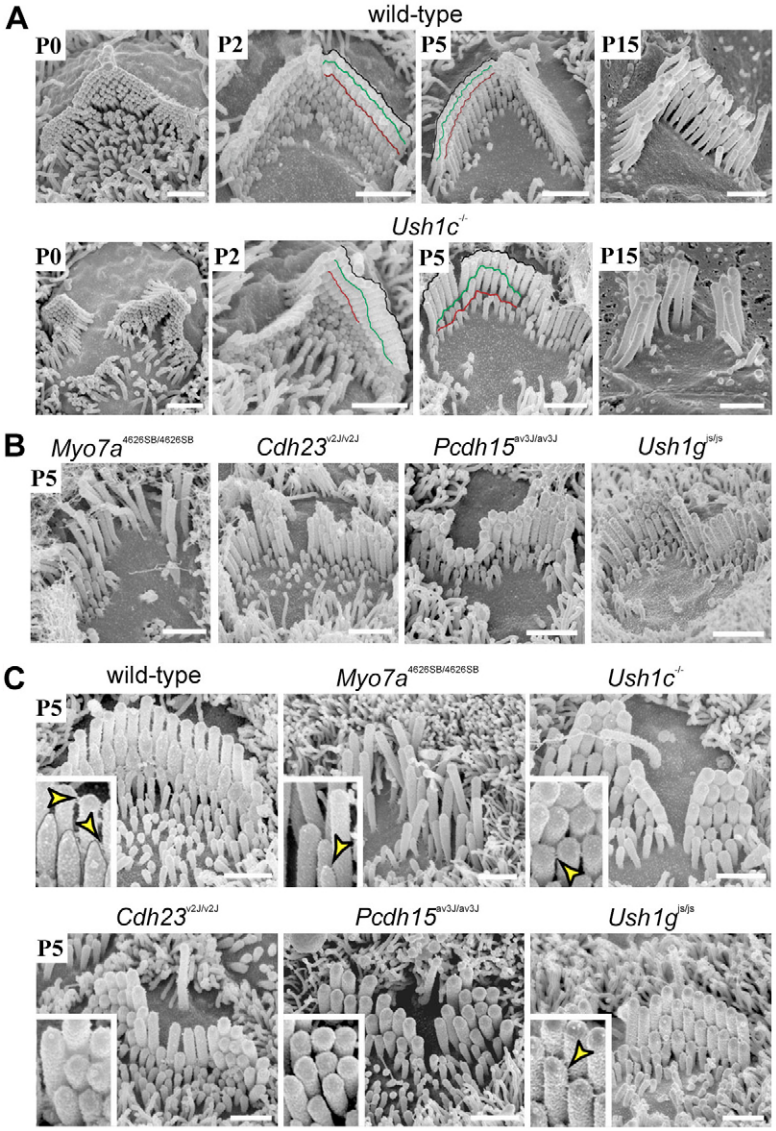

Fig. 6. Elongation and tip defects of stereocilia in *Ush1* mutants during postnatal stages. (**A**) Hair bundle maturation in P0 to P15 wild-type and *Ush1c*$^{-/-}$ OHCs from the end of the apical cochlear turn. At P0, mutant OHC bundles are composed of four to six stereocilia rows almost equal in height, resembling their wild-type counterparts. From this stage onwards, wild-type stereocilia undergo differential growth, depending on the row they belong to. In the absence of harmonin, small and medium stereocilia rows show marked elongation defects from P2 onward, and most of the stereocilia from these rows have disappeared by P15. By contrast, stereocilia from the tall row are of normal length at all stages examined. Note that some small and medium row stereocilia located near clump vertices show some elongation at first (see black, green and red lines running along the tall, medium and small rows of stereocilia, respectively, in P2 and P5 wild-type and mutant OHC bundles). (**B**) OHC bundles of P5 *Myo7a*$^{4626SB/4626SB}$, *Cdh23*$^{v2J/v2J}$, *Pcdh15*$^{av3J/av3J}$ and *Ush1g*$^{js/js}$ mice (view from the end of the apical cochlear turn). Note the abnormal height of many stereocilia of the medium row and the frequent absence of small stereocilia in mutant hair bundles. (**C**) Mid-cochlear IHC bundles of P5 wild-type, *Myo7a*$^{4626SB/4626SB}$, *Ush1c*$^{-/-}$, *Cdh23*$^{v2J/v2J}$, *Pcdh15*$^{av3J/av3J}$ and *Ush1g*$^{js/js}$ mice. As differential elongation occurs, stereocilia of the medium row in wild-type hair bundles acquire a particular prolate shape (see gray lines in the wild-type IHC inset), which could result from tension forces applied to their tip membrane (Rzadzinska et al., 2004). Medium stereocilia of *Ush1* mutant IHCs, however, never display prolate tips (see insets). In addition, apical links (arrowheads) are either absent (*Cdh23*$^{v2J/v2J}$ and *Pcdh15*$^{av3J/av3J}$), or appear sparser (*Myo7a*$^{4626SB/4626SB}$, *Ush1c*$^{-/-}$ and *Ush1g*$^{js/js}$) in the *Ush1* mutants, compared with the controls. Scale bars: 1 μm.

closest microvilli into a polarized, V-shaped stereociliary bundle is still obscure. However, its directional migration towards the cell periphery before any hair bundle is recognizable strongly suggests that it has a leader role in the establishment of hair bundle polarity. Moreover, a lack of polarization or a mispolarization of the stereocilia bundles has recently been reported in mutant hair cells, in which the basal body remained in a central position or was mispositioned, respectively (Jones et al., 2008). In all *Ush1* mouse mutants analyzed here, kinocilia were most frequently mispositioned. Nevertheless, virtually no kinocilia were found at the center or within the medial half of the hair cell apical surface, indicating that the first step of hair bundle polarization is not affected in *Ush1* mutant mice. Moreover, the polarization of Vangl2 and frizzled 3, two essential components of the core PCP pathway (for a review, see Wang and Nathans, 2007) that precedes and participates in the polarized positioning of the kinocilium (Montcouquiol et al., 2003; Wang et al., 2006; Deans et al., 2007), occurred normally at cell-cell junctions in *Ush1* mutant hair cells.

The reorientation step is likely to involve a reorganization of cytoskeletal elements. Although the way it operates is still unknown, it probably involves a connection between the kinociliary basal body and the cell-cell junctions. However, we did not detect harmonin-b, cadherin 23a or protocadherin 15a/b either at the hair cell apical junctions or at the basal body. Instead, our findings suggest that the proper final orientation of the hair bundle requires both the cohesiveness of the stereociliary bundle and its connection to the kinocilium. Indeed, cadherin 23a and protocadherin 15a/b transmembrane isoforms were first detected in the presumptive stereocilia as soon as the kinocilium had reached the cell periphery (at around E16). This indicates that the formation of the stereokinociliary and interstereociliary links made by these cadherins precedes the hair bundle reorientation step. Consistently, interstereociliary and stereokinociliary links have been detected in a majority of hair cells along the cochlea at E17.5 (Goodyear et al., 2005). Moreover, in *Cdh23*$^{v2J/v2J}$ and *Pcdh15*$^{av3J/av3J}$ mutant mice that lack these isoforms, kinocilia were often dissociated from the stereociliary bundles and showed, on average, greater deviations than those of other *Ush1* mutant hair cells. From our results, we can draw the general conclusion that the part of the hair bundle emerging from the apical cell surface, together with the expected cytoskeletal connection between the basal body and cell-cell junctions (Jones et al., 2008), contributes to the determination of the hair bundle final position. Incidentally, the observation that hair bundles in *Cdh23*$^{v2J/v2J}$ and *Pcdh15*$^{av3J/av3J}$ mutant mice often have abnormal

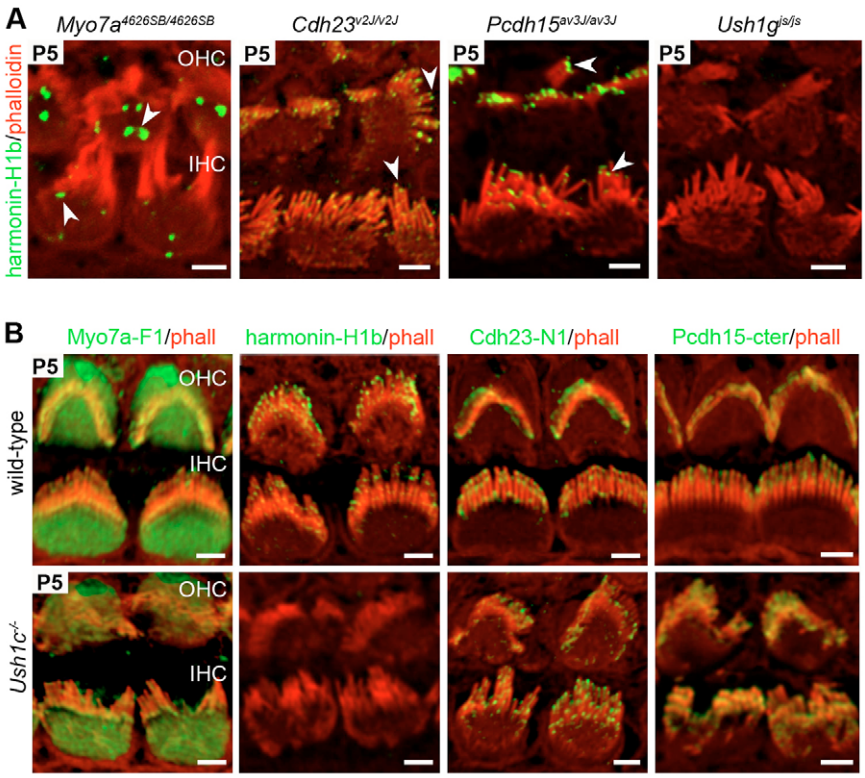

Fig. 7. Mouse Ush1 protein localization in late developing *Ush1* mutant hair bundles. (**A**) Hair bundles of sensory cells from the cochlear basal turn of P5 *Myo7a*$^{4626SB/4626SB}$, *Cdh23*$^{v2J/v2J}$, *Pcdh15*$^{av3J/av3J}$ and *Ush1g*$^{js/js}$ mice were stained with the harmonin-H1b antibody (green) and phalloidin (red). Note again the absence of harmonin-b labeling in hair bundles of *Ush1g*$^{js/js}$ and *Myo7a*$^{4626SB/4626SB}$ mice, and the presence of immunoreactive spots that have increased in number and size since E18.5, in the cuticular plate of the latter mutant (arrowheads). In *Cdh23*$^{v2J/v2J}$ and *Pcdh15*$^{av3J/av3J}$ mice, harmonin-b is also mislocated, as it is still detected at stereocilia tips (arrowheads) instead of near the tip link side attachment point (see wild-type control in B). (**B**) Cochleas of P5 wild-type and *Ush1c*$^{-/-}$ mice were stained with phalloidin (red) and antibodies to myosin VIIa (Myo7a-F1), harmonin-b (harmonin-H1b), cadherin 23a (Cdh23-N1) or protocadherin 15a/b (Pcdh15-cter) (green). The stainings for myosin VIIa, Cdh23-a and Pcdh15-a/b are the same in *Ush1c*$^{-/-}$ and wild-type hair bundles. Scale bars: 2 μm.

'S' or line shapes, together with disconnected kinocilia, also points to an important role of the connection between the kinocilium and stereocilia in the establishment of the normal hair bundle 'V' shape. Finally, because harmonin-b can bind to actin filaments and is colocalized with cadherin 23a and protocadherin 15a/b at stereocilia tips during the initial period of hair bundle development, it is likely to have an essential role in maintaining hair bundle cohesiveness, by anchoring the apical-most cadherin 23- and protocadherin 15-composed links to the stereocilia cytoskeleton.

Based on the concomitance of the hair bundle development and convergent extension processes in the cochlea, we propose the following scenario to account for both hair bundle fragmentation and misorientation in *Ush1* mutants. Traction forces produced within the epithelium by cell intercalations (Keller, 2006) would be transmitted to the growing hair bundles through the apical cell junctions and cytoskeleton. Hair bundle fragmentation would occur as a consequence of the loss of some interstereociliary links, as in the case of *Cdh23*$^{v2J/v2J}$ and *Pcdh15*$^{av3J/av3J}$ mutants, or as a consequence of the weakening of the apical-most links, as in the case of harmonin-deficient, sans-deficient and *Myo7a*$^{4626SB/4626SB}$ mutants. Supporting this proposal, in the vestibule, in which extensive epithelium remodeling by convergent extension does not occur, hair bundles of *Ush1* mutants are rarely fragmented in clumps and display only minor orientation abnormalities, whereas they show significant differential growth defects (G.L., unpublished).

During the intermediate phase of hair bundle morphogenesis, the phenotype of all the *Ush1* mutant mice examined includes abnormal stereociliary elongation. At first glance, the absence of myosin VIIa has an opposite effect on stereocilia growth (increased growth) compared with the absence of any other Ush1 protein (decreased growth). The increased elongation of stereocilia in the absence of myosin VIIa is reminiscent of that induced by mutant forms of myosin IIIa (Schneider et al., 2006). However, the distribution of myosin IIIa, which is restricted to stereocilia tips, indicates a local role for this protein in acting directly on the machinery controlling actin polymerization, whereas the presence of myosin VIIa along the stereocilia shafts rather suggests that it acts as a conveyor of key regulators of actin polymerization towards stereocilia tips. The stereocilia growth defect observed in the other *Ush1* mutants is unprecedented. Indeed, it differs from that observed in mice deficient for myosin XVa, whirlin or espin (Mburu et al., 2003; Probst et al., 1998; Sjostrom and Anniko, 1992; Zheng et al., 2000) in that it spares stereocilia of the tallest row. The concomitant appearance of this defect and switch of the harmonin-b staining from the stereocilia tip to the upper attachment point of the tip link, in conjunction with the involvement of cadherin 23 and protocadherin 15 as tip link components (Ahmed et al., 2006; Kazmierczak et al., 2007; Siemens et al., 2004), strongly suggest that the stereocilia elongation defect of *Ush1* mutants results from insufficient tension forces applied by the tip links on the tips of small and medium stereocilia. Along this line, pulling forces applied to actin filaments have been predicted to control actin polymerization (Hill and Kirschner, 1982), and a mechanism involving formins in this process has been proposed (Kozlov and Bershadsky, 2004). Finally, regarding the differential growth of the tallest stereocilia row, the observation that the length of these stereocilia is not affected when the kinocilium either lacks its axonemal part (Jones et al., 2008) or is entirely disconnected from the stereocilia (*Cdh23*$^{v2J/v2J}$ and *Pcdh15*$^{av3J/av3J}$ mutants, this study), suggests that the kinocilium does not play a crucial role in this process.

Additional lines of evidence suggest that harmonin-b anchors the tip link upper end (likely to be made of cadherin 23) to the stereocilia actin core, hence participating in the transmission of the above-mentioned tension forces. Firstly, direct interactions of harmonin-b with cadherin 23 and F-actin have been shown in vitro (Adato et al., 2005; Boeda et al., 2002; Siemens et al., 2002). Secondly, the harmonin-b immunoreactivity switch does not occur in *Cdh23*$^{v2J/v2J}$ and *Pcdh15*$^{av3J/av3J}$ mice that do not have any detectable tip links.

Thirdly, small and medium stereocilia have oblate-shaped tips in *Cdh23*$^{v2J/v2J}$, *Pcdh15*$^{av3J/av3J}$ and *Ush1c*$^{-/-}$ mutants, instead of the normal prolate-shaped tips that are believed to result from the traction force exerted by the tip link on the apical membrane (Rzadzinska et al., 2004; Prost et al., 2007). Notably, the elongation defect in sans-deficient *Ush1g*$^{js/js}$ mice might result from the absence of harmonin-b, which was never detected in the stereocilia of these mice.

In conclusion, our results on *Ush1* mutant mice shed new light on the cellular mechanisms involved in hair bundle morphogenesis. In particular, they unravel the role of interstereociliary and stereokinociliary links in hair bundle cohesion and orientation at early developmental stages. Moreover, they point to a previously unrecognized role of the tip link in stereocilia differential growth, in addition to its well-established role in mechanoelectrical transduction.

We thank S. Chardenoux, A. David and C. Houdon for technical help; J. Levilliers for help in the preparation of the manuscript; J. Prost for helpful discussion; P. Roux, E. Perret, S. Guadagnini and M.-C. Prévost from the Pasteur Institute Imagopole for their technical advice; and G. Hamard and C. Houbron from the INSERM-Cochin Institute Homologous Recombination core facility for their help in the generation of the *Ush1c*-knockout mouse. G.L. and L.L. received fellowships from the College de France and the Fondation pour la Recherche Médicale, respectively. This work was supported by grants from the Fondation Raymonde et Guy Strittmatter, European Commission FP6 Integrated Project EuroHear (LSHG-CT-2004-512063), A. & M. Suchert-Retina Kontra Blindheit Stiftung, Ernst-Jung Stiftung für Medizin Preis, and the French National Research Agency (ANR-Maladies Rares, ANR-05-MRAR-015-01).

Supplementary material

Supplementary material for this article is available at http://dev.biologists.org/cgi/content/full/135/8/1427/DC1

References

Adato, A., Michel, V., Kikkawa, Y., Reiners, J., Alagramam, K. N., Weil, D., Yonekawa, H., Wolfrum, U., El-Amraoui, A. and Petit, C. (2005). Interactions in the network of Usher syndrome type 1 proteins. *Hum. Mol. Genet.* **14**, 347-356.

Ahmed, Z. M., Riazuddin, S., Bernstein, S. L., Ahmed, Z., Khan, S., Griffith, A. J., Morell, R. J., Friedman, T. B., Riazuddin, S. and Wilcox, E. R. (2001). Mutations of the protocadherin gene PCDH15 cause Usher syndrome type 1F. *Am. J. Hum. Genet.* **69**, 25-34.

Ahmed, Z. M., Riazuddin, S., Ahmad, J., Bernstein, S. L., Guo, Y., Sabar, M. F., Sieving, P., Riazuddin, S., Griffith, A. J., Friedman, T. B. et al. (2003). PCDH15 is expressed in the neurosensory epithelium of the eye and ear and mutant alleles are responsible for both USH1F and DFNB23. *Hum. Mol. Genet.* **12**, 3215-3223.

Ahmed, Z. M., Goodyear, R., Riazuddin, S., Lagziel, A., Legan, P. K., Behra, M., Burgess, S. M., Lilley, K. S., Wilcox, E. R., Riazuddin, S. et al. (2006). The tip-link antigen, a protein associated with the transduction complex of sensory hair cells, is protocadherin-15. *J. Neurosci.* **26**, 7022-7034.

Alagramam, K. N., Murcia, C. L., Kwon, H. Y., Pawlowski, K. S., Wright, C. G. and Woychik, R. P. (2001a). The mouse Ames waltzer hearing-loss mutant is caused by mutation of Pcdh15, a novel protocadherin gene. *Nat. Genet.* **27**, 99-102.

Alagramam, K. N., Yuan, H., Kuehn, M. H., Murcia, C. L., Wayne, S., Srisailpathy, C. R., Lowry, R. B., Knaus, R., Van Laer, L., Bernier, F. P. et al. (2001b). Mutations in the novel protocadherin PCDH15 cause Usher syndrome type 1F. *Hum. Mol. Genet.* **10**, 1709-1718.

Bitner-Glindzicz, M., Lindley, K. J., Rutland, P., Blaydon, D., Smith, V. V., Milla, P. J., Hussain, K., Furth-Lavi, J., Cosgrove, K. E., Shepherd, R. M. et al. (2000). A recessive contiguous gene deletion causing infantile hyperinsulinism, enteropathy and deafness identifies the Usher type 1C gene. *Nat. Genet.* **26**, 56-60.

Boeda, B., El-Amraoui, A., Bahloul, A., Goodyear, R., Daviet, L., Blanchard, S., Perfettini, I., Fath, K. R., Shorte, S., Reiners, J. et al. (2002). Myosin VIIa, harmonin and cadherin 23, three Usher I gene products that cooperate to shape the sensory hair cell bundle. *Embo J.* **21**, 6689-6699.

Bolz, H., von Brederlow, B., Ramirez, A., Bryda, E. C., Kutsche, K., Nothwang, H. G., Seeliger, M., del C-Salcedó Cabrera, M., Vila, M. C., Molina, O. P. et al. (2001). Mutation of CDH23, encoding a new member of the cadherin gene family, causes Usher syndrome type 1D. *Nat. Genet.* **27**, 108-112.

Bork, J. M., Peters, L. M., Riazuddin, S., Bernstein, S. L., Ahmed, Z. M., Ness, S. L., Polomeno, R., Ramesh, A., Schloss, M., Srisailpathy, C. R. et al. (2001). Usher syndrome 1D and nonsyndromic autosomal recessive deafness DFNB12 are caused by allelic mutations of the novel cadherin-like gene CDH23. *Am. J. Hum. Genet.* **68**, 26-37.

Chen, P. and Segil, N. (1999). p27(Kip1) links cell proliferation to morphogenesis in the developing organ of Corti. *Development* **126**, 1581-1590.

Chen, Z. Y., Hasson, T., Kelley, P. M., Schwender, B. J., Schwartz, M. F., Ramakrishnan, M., Kimberling, W. J., Mooseker, M. S. and Corey, D. P. (1996). Molecular cloning and domain structure of human myosin-VIIa, the gene product defective in Usher syndrome 1B. *Genomics* **36**, 440-448.

Cotanche, D. A. and Corwin, J. T. (1991). Stereociliary bundles reorient during hair cell development and regeneration in the chick cochlea. *Hear. Res.* **52**, 379-402.

Dabdoub, A., Donohue, M. J., Brennan, A., Wolf, V., Montcouquiol, M., Sassoon, D. A., Hseih, J. C., Rubin, J. S., Salinas, P. C. and Kelley, M. W. (2003). Wnt signaling mediates reorientation of outer hair cell stereociliary bundles in the mammalian cochlea. *Development* **130**, 2375-2384.

Deans, M. R., Antic, D., Suyama, K., Scott, M. P., Axelrod, J. D. and Goodrich, L. V. (2007). Asymmetric distribution of prickle-like 2 reveals an early underlying polarization of vestibular sensory epithelia in the inner ear. *J. Neurosci.* **27**, 3139-3147.

Denman-Johnson, K. and Forge, A. (1999). Establishment of hair bundle polarity and orientation in the developing vestibular system of the mouse. *J. Neurocytol.* **28**, 821-835.

Di Palma, F., Holme, R. H., Bryda, E. C., Belyantseva, I. A., Pellegrino, R., Kachar, B., Steel, K. P. and Noben-Trauth, K. (2001). Mutations in Cdh23, encoding a new type of cadherin, cause stereocilia disorganization in waltzer, the mouse model for Usher syndrome type 1D. *Nat. Genet.* **27**, 103-107.

el-Amraoui, A., Sahly, I., Picaud, S., Sahel, J., Abitbol, M. and Petit, C. (1996). Human Usher 1B/mouse shaker-1: the retinal phenotype discrepancy explained by the presence/absence of myosin VIIA in the photoreceptor cells. *Hum. Mol. Genet.* **5**, 1171-1178.

Gibson, F., Walsh, J., Mburu, P., Varela, A., Brown, K. A., Antonio, M., Beisel, K. W., Steel, K. P. and Brown, S. D. (1995). A type VII myosin encoded by the mouse deafness gene shaker-1. *Nature* **374**, 62-64.

Goodyear, R. J., Marcotti, W., Kros, C. J. and Richardson, G. P. (2005). Development and properties of stereociliary link types in hair cells of the mouse cochlea. *J. Comp. Neurol.* **485**, 75-85.

Hasson, T., Heintzelman, M. B., Santos-Sacchi, J., Corey, D. P. and Mooseker, M. S. (1995). Expression in cochlea and retina of myosin VIIa, the gene product defective in Usher syndrome type 1B. *Proc. Natl. Acad. Sci. USA* **92**, 9815-9819.

Hill, T. L. and Kirschner, M. W. (1982). Subunit treadmilling of microtubules or actin in the presence of cellular barriers: possible conversion of chemical free energy into mechanical work. *Proc. Natl. Acad. Sci. USA* **79**, 490-494.

Hudspeth, A. J. (1985). Models for mechanoelectrical transduction by hair cells. *Prog. Clin. Biol. Res.* **176**, 193-205.

Johnson, K. R., Gagnon, L. H., Webb, L. S., Peters, L. L., Hawes, N. L., Chang, B. and Zheng, Q. Y. (2003). Mouse models of USH1C and DFNB18: phenotypic and molecular analyses of two new spontaneous mutations of the Ush1c gene. *Hum. Mol. Genet.* **12**, 3075-3086.

Jones, C. and Chen, P. (2007). Planar cell polarity signaling in vertebrates. *BioEssays* **29**, 120-132.

Jones, C., Roper, V. C., Foucher, I., Qian, D., Banizs, B., Petit, C., Yoder, B. and Chen, P. (2008). Ciliary proteins link basal body polarization to planar cell polarity regulation. *Nat. Genet.* **40**, 69-77.

Kaltenbach, J. A., Falzarano, P. R. and Simpson, T. H. (1994). Postnatal development of the hamster cochlea. II. Growth and differentiation of stereocilia bundles. *J. Comp. Neurol.* **350**, 187-198.

Kazmierczak, P., Sakaguchi, H., Tokita, J., Wilson-Kubalek, E. M., Milligan, R. A., Müller, U. and Kachar, B. (2007). Cadherin 23 and protocadherin 15 interact to form tip-link filaments in sensory hair cells. *Nature* **449**, 87-91.

Keller, R. (2006). Mechanisms of elongation in embryogenesis. *Development* **133**, 2291-2302.

Kikkawa, Y., Shitara, H., Wakana, S., Kohara, Y., Takada, T., Okamoto, M., Taya, C., Kamiya, K., Yoshikawa, Y., Tokano, H. et al. (2003). Mutations in a new scaffold protein Sans cause deafness in Jackson shaker mice. *Hum. Mol. Genet.* **12**, 453-461.

Kitamura, K., Kakoi, H., Yoshikawa, Y. and Ochikubo, F. (1992). Ultrastructural findings in the inner ear of Jackson shaker mice. *Acta Otolaryngol.* **112**, 622-627.

Kozlov, M. M. and Bershadsky, A. D. (2004). Processive capping by formin suggests a force-driven mechanism of actin polymerization. *J. Cell Biol.* **167**, 1011-1017.

Lagziel, A., Ahmed, Z. M., Schultz, J. M., Morell, R. J., Belyantseva, I. A. and Friedman, T. B. (2005). Spatiotemporal pattern and isoforms of cadherin 23 in wild type and waltzer mice during inner ear hair cell development. *Dev. Biol.* **280**, 295-306.

Lim, D. J. and Anniko, M. (1985). Developmental morphology of the mouse inner ear. A scanning electron microscopic observation. *Acta Otolaryngol.* Suppl. **422**, 1-69.

Mburu, P., Mustapha, M., Varela, A., Weil, D., El-Amraoui, A., Holme, R. H., Rump, A., Hardisty, R. E., Blanchard, S., Coimbra, R. S. et al. (2003). Defects in whirlin, a PDZ domain molecule involved in stereocilia elongation, cause deafness in the whirler mouse and families with DFNB31. *Nat. Genet.* **34**, 421-428.

Michalski, N., Michel, V., Bahloul, A., Lefevre, G., Barral, J., Yagi, H., Chardenoux, S., Weil, D., Martin, P., Hardelin, J. P. et al. (2007). Molecular characterization of the ankle-link complex in cochlear hair cells and its role in the hair bundle functioning. *J. Neurosci.* **27**, 6478-6488.

Michel, V., Goodyear, R. J., Weil, D., Marcotti, W., Perfettini, I., Wolfrum, U., Kros, C. J., Richardson, G. P. and Petit, C. (2005). Cadherin 23 is a component of the transient lateral links in the developing hair bundles of cochlear sensory cells. *Dev. Biol.* **280**, 281-294.

Montcouquiol, M., Rachel, R. A., Lanford, P. J., Copeland, N. G., Jenkins, N. A. and Kelley, M. W. (2003). Identification of Vangl2 and Scrb1 as planar polarity genes in mammals. *Nature* **423**, 173-177.

Pawlowski, K. S., Kikkawa, Y. S., Wright, C. G. and Alagramam, K. N. (2006). Progression of inner ear pathology in Ames waltzer mice and the role of protocadherin 15 in hair cell development. *J. Assoc. Res. Otolaryngol.* **7**, 83-94.

Probst, F. J., Fridell, R. A., Raphael, Y., Saunders, T. L., Wang, A., Liang, Y., Morell, R. J., Touchman, J. W., Lyons, R. H., Noben-Trauth, K. et al. (1998). Correction of deafness in shaker-2 mice by an unconventional myosin in a BAC transgene. *Science* **280**, 1444-1447.

Prost, J., Barbetta, C. and Joanny, J. F. (2007). Dynamical control of the shape and size of stereocilia and microvilli. *Biophys. J.* **93**, 1124-1133.

Reiners, J., Reidel, B., El-Amraoui, A., Boeda, B., Huber, I., Petit, C. and Wolfrum, U. (2003). Differential distribution of harmonin isoforms and their possible role in Usher-1 protein complexes in mammalian photoreceptor cells. *Invest. Ophthalmol. Vis. Sci.* **44**, 5006-5015.

Reiners, J., Marker, T., Jurgens, K., Reidel, B. and Wolfrum, U. (2005). Photoreceptor expression of the Usher syndrome type 1 protein protocadherin 15 (USH1F) and its interaction with the scaffold protein harmonin (USH1C). *Mol. Vis.* **11**, 347-355.

Rzadzinska, A. K., Schneider, M. E., Davies, C., Riordan, G. P. and Kachar, B. (2004). An actin molecular treadmill and myosins maintain stereocilia functional architecture and self-renewal. *J. Cell Biol.* **164**, 887-897.

Rzadzinska, A. K., Derr, A., Kachar, B. and Noben-Trauth, K. (2005). Sustained cadherin 23 expression in young and adult cochlea of normal and hearing-impaired mice. *Hear. Res.* **208**, 114-121.

Schneider, M. E., Dose, A. C., Salles, F. T., Chang, W., Erickson, F. L., Burnside, B. and Kachar, B. (2006). A new compartment at stereocilia tips defined by spatial and temporal patterns of myosin IIIa expression. *J. Neurosci.* **26**, 10243-10252.

Senften, M., Schwander, M., Kazmierczak, P., Lillo, C., Shin, J. B., Hasson, T., Geleoc, G. S., Gillespie, P. G., Williams, D., Holt, J. R. et al. (2006). Physical and functional interaction between protocadherin 15 and myosin VIIa in mechanosensory hair cells. *J. Neurosci.* **26**, 2060-2071.

Sher, A. E. (1971). The embryonic and postnatal development of the inner ear of the mouse. *Acta Otolaryngol.* Suppl. **285**, 1-77.

Siemens, J., Kazmierczak, P., Reynolds, A., Sticker, M., Littlewood-Evans, A. and Muller, U. (2002). The Usher syndrome proteins cadherin 23 and harmonin form a complex by means of PDZ-domain interactions. *Proc. Natl. Acad. Sci. USA* **99**, 14946-14951.

Siemens, J., Lillo, C., Dumont, R. A., Reynolds, A., Williams, D. S., Gillespie, P. G. and Muller, U. (2004). Cadherin 23 is a component of the tip link in hair-cell stereocilia. *Nature* **428**, 950-955.

Sjostrom, B. and Anniko, M. (1992). Genetically induced inner ear degeneration. A structural and functional study. *Acta Otolaryngol.* Suppl. **493**, 141-146.

Verpy, E., Leibovici, M., Zwaenepoel, I., Liu, X. Z., Gal, A., Salem, N., Mansour, A., Blanchard, S., Kobayashi, I., Keats, B. J. et al. (2000). A defect in harmonin, a PDZ domain-containing protein expressed in the inner ear sensory hair cells, underlies Usher syndrome type 1C. *Nat. Genet.* **26**, 51-55.

Wang, Y. and Nathans, J. (2007). Tissue/planar cell polarity in vertebrates: new insights and new questions. *Development* **134**, 647-658.

Wang, Y., Guo, N. and Nathans, J. (2006). The role of Frizzled3 and Frizzled6 in neural tube closure and in the planar polarity of inner-ear sensory hair cells. *J. Neurosci.* **26**, 2147-2156.

Weil, D., Blanchard, S., Kaplan, J., Guilford, P., Gibson, F., Walsh, J., Mburu, P., Varela, A., Levilliers, J., Weston, M. D. et al. (1995). Defective myosin VIIA gene responsible for Usher syndrome type 1B. *Nature* **374**, 60-61.

Weil, D., El-Amraoui, A., Masmoudi, S., Mustapha, M., Kikkawa, Y., Laine, S., Delmaghani, S., Adato, A., Nadifi, S., Zina, Z. B. et al. (2003). Usher syndrome type I G (USH1G) is caused by mutations in the gene encoding SANS, a protein that associates with the USH1C protein, harmonin. *Hum. Mol. Genet.* **12**, 463-471.

Wilson, S. M., Householder, D. B., Coppola, V., Tessarollo, L., Fritzsch, B., Lee, E. C., Goss, D., Carlson, G. A., Copeland, N. G. and Jenkins, N. A. (2001). Mutations in Cdh23 cause nonsyndromic hearing loss in waltzer mice. *Genomics* **74**, 228-233.

Zheng, L., Sekerkova, G., Vranich, K., Tilney, L. G., Mugnaini, E. and Bartles, J. R. (2000). The deaf jerker mouse has a mutation in the gene encoding the espin actin-bundling proteins of hair cell stereocilia and lacks espins. *Cell* **102**, 377-385.

Zine, A. and Romand, R. (1996). Development of the auditory receptors of the rat: a SEM study. *Brain Res.* **721**, 49-58.

Zwaenepoel, I., Verpy, E., Blanchard, S., Meins, M., Apfelstedt-Sylla, E., Gal, A. and Petit, C. (2001). Identification of three novel mutations in the USH1C gene and detection of thirty-one polymorphisms used for haplotype analysis. *Hum. Mutat.* **17**, 34-41.